



# Assessment of Thermal Stratification in Versatile Test Reactor Transients

March 2022

*Changing the World's Energy Future*

SuJong Yoon, Justin W. Thomas, Thomas H. Fanning, Tyler S. Sumner



*INL is a U.S. Department of Energy National Laboratory operated by Battelle Energy Alliance, LLC*

#### **DISCLAIMER**

This information was prepared as an account of work sponsored by an agency of the U.S. Government. Neither the U.S. Government nor any agency thereof, nor any of their employees, makes any warranty, expressed or implied, or assumes any legal liability or responsibility for the accuracy, completeness, or usefulness, of any information, apparatus, product, or process disclosed, or represents that its use would not infringe privately owned rights. References herein to any specific commercial product, process, or service by trade name, trade mark, manufacturer, or otherwise, does not necessarily constitute or imply its endorsement, recommendation, or favoring by the U.S. Government or any agency thereof. The views and opinions of authors expressed herein do not necessarily state or reflect those of the U.S. Government or any agency thereof.

# **Assessment of Thermal Stratification in Versatile Test Reactor Transients**

**SuJong Yoon, Justin W. Thomas, Thomas H. Fanning, Tyler S. Sumner**

**March 2022**

**Idaho National Laboratory  
Idaho Falls, Idaho 83415**

**<http://www.inl.gov>**

**Prepared for the  
U.S. Department of Energy  
Under DOE Idaho Operations Office  
Contract DE-AC07-05ID14517**

# ASSESSMENT OF THERMAL STRATIFICATION IN VERSATILE TEST REACTOR TRANSIENTS

**SuJong Yoon\***

Idaho National Laboratory

2525 Fremont Ave., Idaho Falls, ID 83415

[sujong.yoon@inl.gov](mailto:sujong.yoon@inl.gov)

**Justin W. Thomas, Tyler S. Sumner, and Thomas H. Fanning**

Argonne National Laboratory

9700 South Cass Avenue, Lemont, IL 60439

[jthomas@anl.gov](mailto:jthomas@anl.gov); [tsumner@anl.gov](mailto:tsumner@anl.gov); [fanning@anl.gov](mailto:fanning@anl.gov)

## ABSTRACT

The Versatile Test Reactor (VTR) is a fast-spectrum test reactor currently being developed in the United States (U.S.) under the direction of the U.S. Department of Energy (DOE). The conceptual design of the 300 MWth pool-type sodium-cooled fast reactor (SFR) has been led by the U.S. National Laboratories in collaboration with General Electric-Hitachi and Bechtel National Inc. Safety performance analysis for the VTR conceptual design is being performed with the SAS4A/SASSYS-1 liquid-metal reactor safety analysis code system. Since the current model of the VTR employs a simple perfect mixing model for large plena—such as the hot pool, it is not able to predict temperature variations that may develop during the transient. Prior work simulating the response of SFRs to postulated events like the protected station blackout (PSBO) has shown that the phenomenon of thermal stratification, where stable thermal layers accumulate in the hot pool, may delay the transition to natural circulation, and thus impact the predicted transient progression. Thus, an effort has begun to model this transient by integrating a computational fluid dynamics (CFD) model of the hot pool into the SAS4A/SASSYS-1 model of the Primary Heat Transport System during the simulation of the PSBO event. A three-dimensional volume-of-fluid CFD model of the VTR hot pool has been developed for the co-simulation of SAS4A/SASSYS-1 with CFD. In this work, the standalone SAS4A/SASSYS-1 calculation and the standalone CFD calculation based on the SAS4A/SASSYS-1 calculation result were produced on Idaho National Laboratory's (INL's) high performance computing (HPC) cluster, SAWTOOTH. At this time, only the standalone CFD and SAS4A/SASSYS-1 simulation results are provided.

## KEYWORDS

SFR Safety, SAS4A/SASSYS-1, SYSTH-CFD Coupling, Thermal Stratification

## 1. INTRODUCTION

The safety design strategy of the Versatile Test Reactor (VTR) includes a defense-in-depth approach that utilizes passive safety systems to provide additional margins for protecting workers and the public from relatively low frequency events [1]. The safety performance for events that feature loss of forced circulation, notably the protected station blackout (PSBO), is enhanced by the establishment of buoyancy-driven natural circulation of sodium coolant to transport decay heat from the core, where it is ultimately rejected to the reactor vessel auxiliary cooling system (RVACS). This transient performance of the VTR design during

such events is being modeled primarily with the SAS4A/SASSYS-1 (a.k.a. “SAS”) v5.4 fast reactor safety analysis code [2]. The VTR SAS4A/SASSYS-1 model represents the reactor core, primary and intermediate heat transport systems, RVACS, and an assumed reactor protection system (RPS) [3]. Such a simplified model cannot capture the multidimensional phenomena that are observed in large pools under such transient conditions. Thermal stratification in the hot pool of pool-type SFRs under low-flow conditions has been shown to impede the establishment of natural circulation, elevating core temperatures relative to the predictions of a perfect mixing model [4]. There has been significant prior work to model these phenomena in SFRs [5], as well as international collaborations to validate such models [6, 7].

The objective of this study is to assess the influence of thermal stratification in the VTR hot pool on the transient response of the postulated PSBO event. This is being explored initially with a CFD model of the hot pool employing the STAR-CCM+ code [8]. The time-dependent boundary conditions are obtained from the standalone calculations of SAS4A/SASSYS-1. This will provide an initial assessment of the extent of thermal stratification. To assess the influence on the overall transient progression, SAS4A/SASSYS-1 and CFD models will be coupled together employing similar techniques as published previously [4, 9]. This analysis is underway, but results are not currently available for this publication.

## 2. SAS4A/SASSYS-1 MODEL OF THE PSBO TRANSIENT

The SAS model of the core employs 26 representative channels—each with a single-pin and surrounding coolant—to represent the 313 core subassemblies at beginning-of-cycle conditions. Of these 313 subassemblies, 66 are fuel assemblies, and are represented by 16 of the channels. This includes one channel to represent the fuel assembly with the peak power-to-flow ratio, and six more for its neighbors. The remaining channels are used to represent the control and safety rods, reflector assemblies, shield, and experimental locations where irradiation tests are conducted. The model employs 1-D single-phase axial coolant thermal-hydraulics connected to a 1-D radial solid conduction model through the fuel, cladding, and associated structure to predict transient temperatures. A point kinetics model is employed to predict changes in the core power prior to scram, which accounts for fuel Doppler, coolant density, fuel pin axial expansion, core radial expansion, control rod driveline expansion, and reactor vessel expansion reactivity feedback effects. Decay heat is modeled using the American Nuclear Society (ANS) decay heat standard for light water reactors (LWRs), with specifications for the fraction of power produced by each fissile isotope.

Outside the core, the SAS model represents the primary and secondary sodium heat transport systems, as a network of 1-D flow elements that are connected to 0-D compressible volumes. The flow elements include component models for flow and/or heat transfer in the primary and secondary pumps, intermediate heat exchanger (IHX), sodium-to-air heat exchangers, and the RVACS. The compressible volumes represent plena, including large volumes of coolant such as the hot and cold pools, using a perfect mixing model, where the outlet temperature at a point in time is the mixed mean temperature of the volume.

The PSBO event is assumed to be initiated by loss of electrical power to all plant systems, resulting in the loss of forced circulation in the primary and secondary coolant loops. The heat rejection through the sodium-to-air heat exchangers is also assumed to decrease to zero. Upon trip of the electromagnetic pumps, there is an immediate reduction in flow rate to 60% of its nominal value, followed by a 12 second halving time. The reactor protection system is assumed to scram the reactor once the power-to-flow ratio exceeds 115% of its nominal value, which occurs almost immediately after the sodium pumps trip. The SAS4A/SASSYS-1 model predicts that the peak fuel, cladding, and core coolant temperatures occur during the initial phase of the transient, prior to scram, where the flow rate is reduced, but the reactor power is close to its nominal value [2].

With a perfect mixing model in the hot pool, the IHX inlet temperature is predicted to decrease immediately in response to the reduction in core outlet temperature following a scram. However, in the absence of forced flow from the primary pumps, several minutes may be required for the cold front to travel approximately 8.5 m from the core outlet to the IHX inlet window. In the meantime, coolant temperatures in the IHX, which serves as the heat sink for the primary loop, exceed the core outlet temperature, thus impeding natural circulation. This delay in natural circulation may not influence the peak core temperatures, which are predicted to occur in the initial phase of the transient prior to scram but may cause these temperatures to remain elevated for a longer duration compared to the predictions of the perfect mixing model.

To evaluate the influence of thermal stratification on the response to the PSBO transient, the results of the mass flow rate and temperature at each connection to the hot pool at each time step will be provided to the CFD model for boundary conditions. The CFD model will then provide an updated prediction of the IHX inlet temperature, which is anticipated to remain elevated above the corresponding predictions of the perfect mixing model in SAS. The significance of this delay will motivate further exploration by coupling the SAS and CFD models directly.

### 3. CFD MODEL DESCRIPTION

The CFD model of the hot pool was developed using the commercial CFD software, STAR-CCM+ v15.06. The geometry was developed with a negative volume extraction method based on a 3D computer-aided design (CAD) drawing of the VTR conceptual design, as shown in Fig. 1. The geometry includes the fluid inside the upper plenum, surrounding the housings for the primary pumps, IHXs, and the upper internal structure (UIS). The hexagonal lattice of the core outlet includes the outlet of 313 core assemblies that are grouped into the 26 channels employed by the SAS model. The initial conditions of these channels are determined from the SAS steady-state predictions. The fluid domain is part-based meshed with polyhedral cells and three prism boundary layers near the wall. The total number of computational cells is approximately 32 M. The mesh structure on the cross-section highlighted by red in the geometry scenes (Fig. 1-(a), (b) and (c) is illustrated in Fig. 1-(d). In the top region, the mesh was refined locally to better capture the interface between the liquid sodium and the Argon cover gas.

The model contains two fluids—liquid sodium as a coolant and Argon gas as a compressible cover gas layer. The volume-of-fluid method [8] with a high-resolution interface capturing (HRIC) convection scheme [10] was employed to take account of the two fluids. The elevation of liquid sodium was specified as an initial condition. The sharpening factor and angle factor of the HRIC scheme are 0.5 and 0.05, respectively.

The temperature-dependent liquid sodium density, dynamic viscosity, thermal conductivity, and specific heat is specified by polynomial functions that are consistent with the corresponding properties employed by the SAS code. Argon cover gas is specified as ideal gas.

The realizable k- $\epsilon$  two-layer turbulence model [11] was selected for the Reynolds-Averaged Navier-Stokes method. Buoyancy forces are accounted for by the Boussinesq model. A second-order convection scheme is used for both segregated flow and segregated temperature solvers.

In this study, “mass flow inlet” boundary conditions are employed at all flow boundaries, including the 26 channel groups at the core outlet and the two IHX inlet windows. At these boundary conditions, time-dependent mass flow rate and temperature are imposed using tabular data extracted from the SAS calculations. In the SAS predictions, the mass flow rate at the IHX inlet window is directed outward (i.e., into the IHX), and therefore, the specified temperature is ignored.

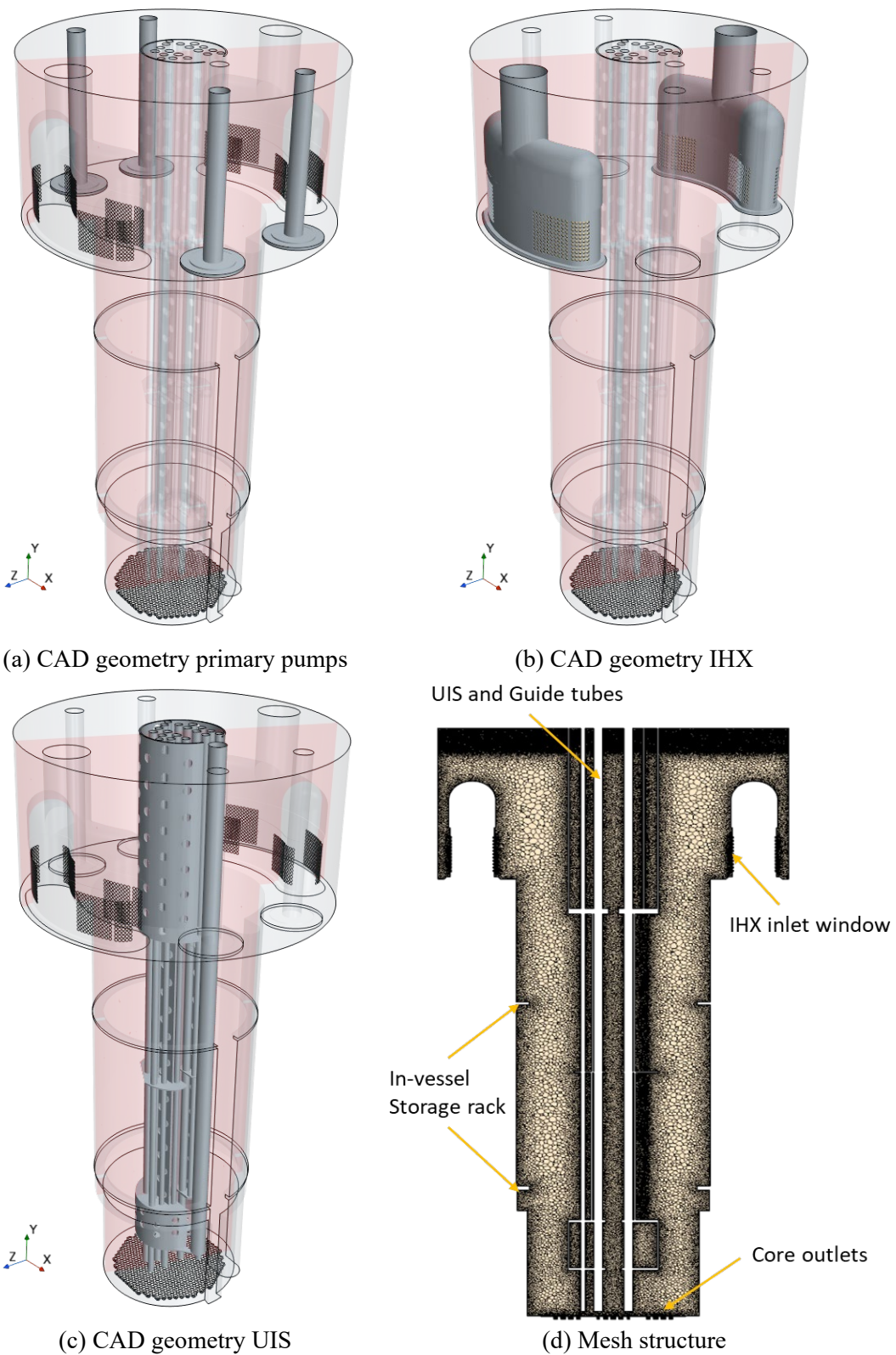


Figure 1. VTR Upper Plenum Geometry and Mesh Structure.

Simulations were performed on 1,440 cores of Idaho National Laboratory's (INL's) high performance computing (HPC) cluster, SAWTOOTH. The SAWTOOTH cluster consists of 2,079 compute nodes. Each node of SAWTOOTH has 48 cores and 192 gigabytes (GB) of memory. Some nodes also have four NVIDIA V100 graphics processing units (GPUs) and an additional 192 GB of random-access memory (RAM) for a total of 384 GB of memory. The total memory of SAWTOOTH is 404 terabytes (TB).

## 4. RESULTS AND DISCUSSION

Prior to the coupled calculation of SAS with the CFD, the standalone SAS calculation and standalone CFD calculation based on the SAS calculation were carried out to investigate the thermal-hydraulic characteristics in the VTR upper pool.

### 4.1. SAS4A/SASSYS-1 Standalone Calculation

The PSBO transient is characterized by a rapid reduction in forced flow rate, which activates the RPS to initiate a scram. The SAS predictions for core flow rate and power, relative to their initial values at full power and flow conditions, are plotted in Fig. 2. For the first second of the transient, the relative flow rate is below that of the relative power, causing an increase in coolant temperatures in the core, which propagates to the primary heat transport system. Predicted evolutions of the coolant temperatures are plotted in Fig. 3, including the maximum coolant temperature in the channel with the highest power-to-flow ratio (red), the average outlet temperature of all core subassemblies (purple), and the IHX inlet temperature (green).

The peak core temperature increases quickly in response to the reduced flow rate, as the response is immediately adjacent to the high-powered fuel pins. The average core outlet temperature response is mitigated by relatively cool subassemblies, including reflectors and shields. The IHX inlet temperature, which is equal to the mean hot pool temperature, is further mitigated by the thermal inertia of the large sodium inventory. Although slower to respond than the temperatures in the core, this response starts within only a few seconds of transient initiation because of the treatment from the perfect mixing model.

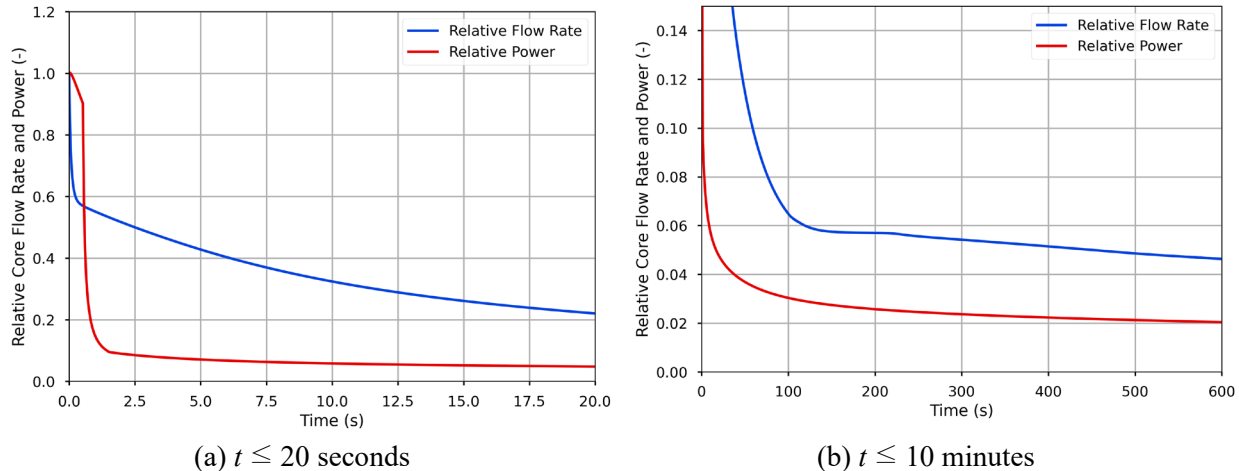


**Figure 2. Relative Core Flow Rate and Power during the PSBO Transient.**

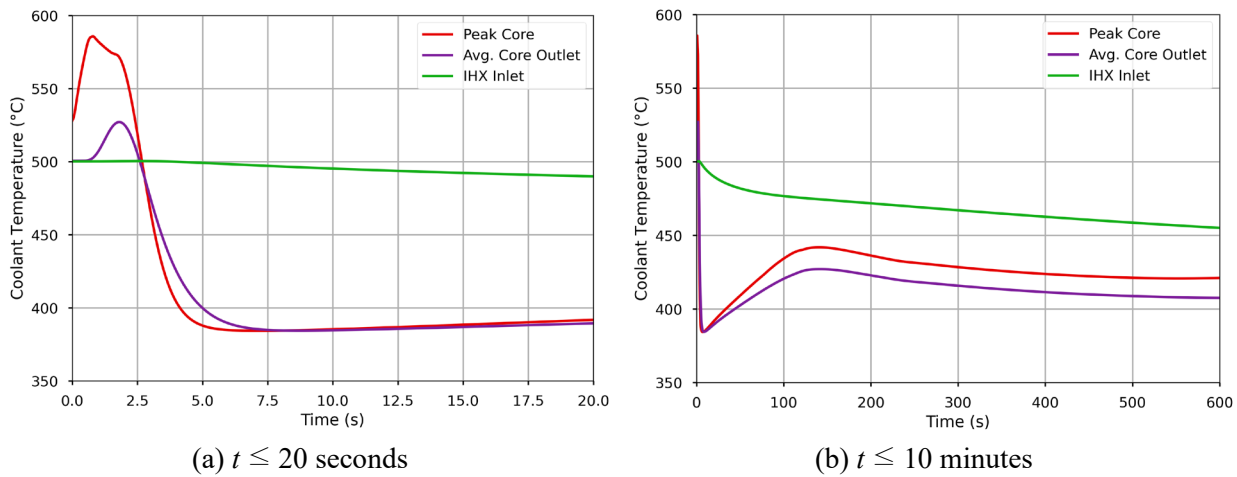


**Figure 3. SAS Predictions of Coolant Temperature during the PSBO Transient.**

#### 4.2. CFD Calculation based on SAS4A/SASSYS-1 Calculation

The core outlets of VTR are the inlet boundaries of the VTR upper pool model. The time-dependent mass flow rate and temperature conditions imposed on the inlet boundaries of the CFD model were provided from the SAS4A/SASSYS-1 calculation. Figures 4 and 5 show the transient temperature and absolute pressure distributions in the VTR upper pool during the PSBO transient, respectively. At the initial steady-state condition ( $t = 0$  sec), the temperature gradient along the axial direction was small ( $< 3^\circ\text{C}$ ). In the early stage of transient ( $t < 100$  sec), the temperature and flow rate of core outlets decreased drastically. These variations of the coolants from core outlet resulted in the complicated flow mixing at the bottom region of the upper pool. After the flow rate of core outlet flows decreased down to 100 kg/s, it began to decrease smoothly, and the axial heat conduction became a dominant heat transfer mechanism in the upper pool. The IHX inlet windows temperature began to be influenced by the cold temperature coolant 300 seconds after the transient initiated. The cold temperature coolant reached the bottom of IHX windows at 400 seconds. The pressure in the upper pool also decreased slightly during this transient.

Figure 6 shows the comparison of IHX inlet temperatures calculated by SAS and CFD. The temperatures at IHX inlet windows in the CFD calculation was not changed significantly up to 300 seconds, whereas it began to decrease as soon as the transient initiated in the SAS calculation with the perfect mixing model. The IHX temperatures calculated by CFD and SAS intersected at 470 seconds. Hence, the core inlet temperature in the standalone SAS calculation was underpredicted for 470 seconds after the transient occurred.

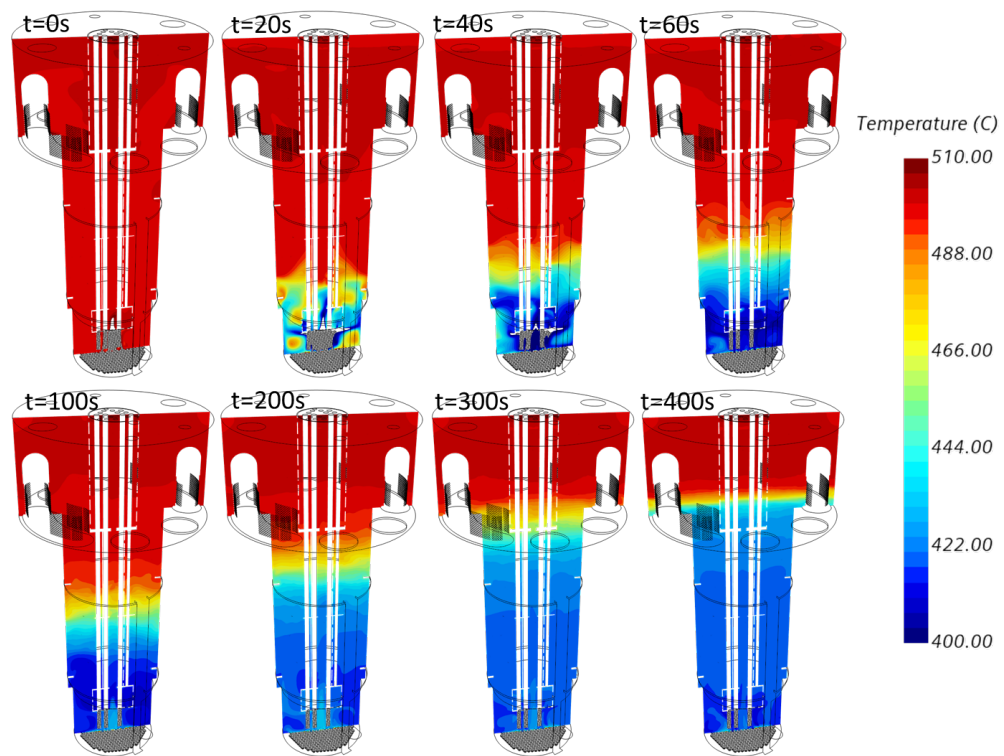


**Figure 4. Transient Temperature Distribution in VTR Upper Pool during the PSBO Transient.**

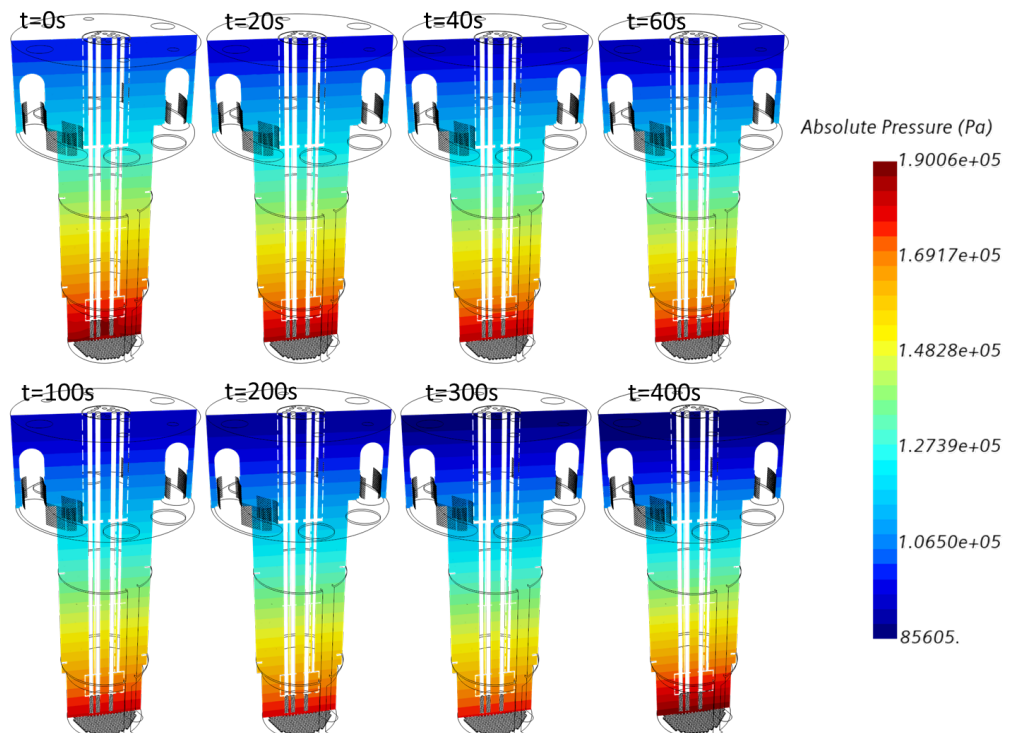


**Figure 5. Transient Absolute Pressure Distribution in VTR Upper Pool during the PSBO Transient.**

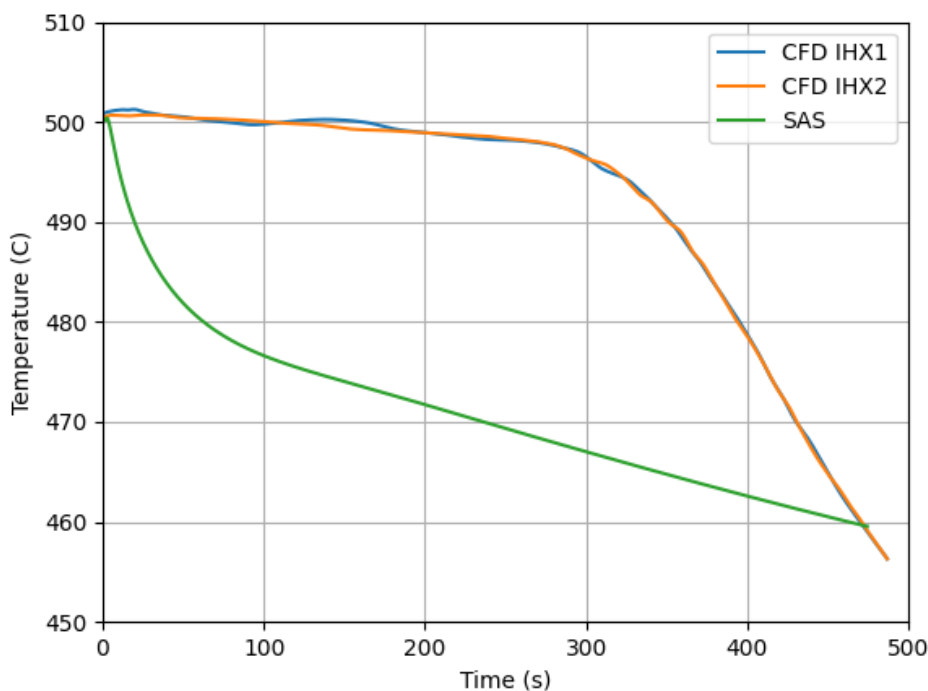


**Figure 6. Comparison of Transient Coolant Temperature at the IHX Inlet Window Calculated by SAS and CFD.**

## 5. CONCLUSIONS

The system thermal-hydraulic calculation of the VTR system and CFD calculation of the hot upper pool of the VTR were produced, and coupled simulations are planned. The temperatures at the IHX inlet window in the hot pool calculated by the 3D CFD model and by the perfect mixing model in SAS showed a significant discrepancy during the transient. In the CFD calculation, stable thermal stratified layers develop as the coolant entering the bottom of the hot pool from the core outlet is significantly cooler than the coolant that was already present prior to the scram. Because of the flow coast down, significant time is required for the relatively cool layer to be advected to the IHX inlet window near the top of the hot pool. The perfect mixing model in SAS predicts an immediate decrease in the IHX inlet temperature once the transient is initiated, whereas the IHX inlet window temperature in CFD remains quite high for the first five minutes of the transient. In a further study, the standalone calculations performed in this work will be compared to the co-simulation result to investigate the coupling effect.

## ACKNOWLEDGMENTS

The work reported in this summary is the result of studies supporting a VTR conceptual design, cost, and schedule estimate for DOE-NE to make a decision on procurement. As such, it is preliminary. INL and Argonne National Laboratory's (ANL's) works were supported by DOE's Office of Nuclear Energy, under contracts DE-AC07-05ID14517 and DE-AC02-06CH11357, respectively. Simulations described in this paper employed the resources of INL's HPC.

## REFERENCES

1. D. Gerstner, J. Andrus, D. Grabaskas, M. Bucknor (2019). "Safety Design Strategy for the Versatile Test Reactor," Transactions of the American Nuclear Society, 2019 ANS Winter Meeting, Washington, DC, USA, November 2019, Vol. 121 (1), pp. 1383-1386.
2. T.H. Fanning, A.J. Brunett, and T. Sumner (eds.) (2017). "The SAS4A/SASSYS-1 Safety Analysis Code System," ANL/NE-16/19, Nuclear Engineering Division, Argonne National Laboratory, March 31, 2017.
3. T.S. Sumner, T.H. Fanning, and J.W. Thomas (2020). "Safety Analysis of the Conceptual Versatile Test Reactor Design", Transactions of the American Nuclear Society, 2020 ANS Virtual Winter Meeting, November 16-19, 2020, Vol. 123, pp. 981-992.
4. T.H. Fanning and J.W. Thomas (2011). "Integration of CFD into Systems Analysis Codes for Modeling Thermal Stratification during SFR Transients," The 14th International Topical Meeting on Nuclear Reactor Thermal-hydraulics (NURETH-14), Toronto, Ontario, Canada, September 25-30, 2011, Paper 398.
5. Z. Wu, C. Lu, S. Morgan, S. Bilbao y Leon, M. Bucknor (2020). "A Status Review on the Thermal Stratification Modeling Methods for Sodium-cooled Fast Reactors," *Progress in Nuclear Energy*, 125, 103369.
6. S. Yoshikawa and M. Minami (2009). "Data Description for Coordinated Research Project on Benchmark Analyses of Sodium Natural Convection in the Upper Plenum of the MONJU Reactor Vessel under Supervisory of Technical Working Group on Fast Reactors, International Atomic Energy Agency," JAEA-Data/Code 2008-024, Japan Atomic Energy Agency.
7. V. Narcisi, F. Giannetti, A. del Nevo, F. Alcaro, X. Wang, A. Kraus, A. Brunett, J. Thomas, N. Girault, B. Grosjean, et al. (2019). "System thermal-hydraulic modelling of the phénix dissymmetric test benchmark," *Nuclear Engineering and Design*, 353, 110272.
8. Siemens PLM Software (2020). "STAR-CCM+ Documentation."
9. J.W. Thomas, S. Passerini, R.B. Vilim, and D.G. Holler (2018). "Preliminary Analysis of the MONJU Turbine Trip Test using a Coupled CFD/System Code Model," The 12th International Topical Meeting on Nuclear Reactor Thermal-Hydraulics, Operation and Safety (NUTHOS-12), Qingdao, China, October 14-18, 2018, paper 65552.
10. S. Muzaferija and M. Peric (1999). "Computation of free surface flows using interface-tracking and interface-capturing methods," Chap. 2 in O. Mahrenholtz and M. Markiewicz (eds.), *Nonlinear Water Wave Interaction*, Computational Mechanics Publications, WIT Press, Southampton, UK.
11. T.-H. Shih, W.W. Liou, A. Shabbir, Z. Yang, and J. Zhu (1994). "A New k- $\epsilon$  Eddy Viscosity Model for High Reynolds Number Turbulent Flows -- Model Development and Validation," NASA TM 106721.